

See discussions, stats, and author profiles for this publication at:  
<http://www.researchgate.net/publication/249899391>

# Mechanism of Illitization of Bentonites in the Geothermal Field of Milos Island Greece: Evidence Based on Mineralogy, Chemistry, Particle Thickness and Morphology

ARTICLE *in* CLAYS AND CLAY MINERALS · OCTOBER 1995

Impact Factor: 1.23 · DOI: 10.1346/CCMN.1995.0430507

---

CITATIONS

11

---

READS

20

1 AUTHOR:



G.E. Christidis

Technical University of Crete

48 PUBLICATIONS 690 CITATIONS

SEE PROFILE

# MECHANISM OF ILLITIZATION OF BENTONITES IN THE GEOHERMAL FIELD OF MILOS ISLAND GREECE: EVIDENCE BASED ON MINERALOGY, CHEMISTRY, PARTICLE THICKNESS AND MORPHOLOGY

GEORGE E. CHRISTIDIS

Technical University of Crete, Department of Mineral Resources Engineering, 73133 Chania, Crete, Greece

**Abstract**—Hydrothermal alteration has caused illitization along a 40m vertical profile in the Tsantilis bentonite deposit, Eastern Milos, Greece which consists principally of a Wyoming-type montmorillonite and authigenic K-feldspar. The product K-bentonite which contains illite/smectite, kaolinite, K-feldspar, quartz, sulphates and sulphides exhibits an unusual tendency for increase of expandability with depth.

Mineralogy and I/S textures were determined with X-ray diffraction and SEM and TEM methods respectively and chemistry using X-ray fluorescence. Illitization is characterized by a 5- to 6-fold increase of K and release of Si, Fe, Mg Na, and Ca from the parent rock, indicating a K-influx (K-metasomatism) in the system.

The I/S particle morphology is characterized by both flaky and lath-like particles, the former dominating in the range 100–50% expandable layers (R0 ordering) and the latter in the range 50–10% expandable layers (R1 and R > 1 ordering). Flaky particles are also abundant in samples with R1 ordering and abundant kaolinite, indicating that the latter might affect illitization. The I/S particles are classified in populations with thickness multiples of 10 Å, their thickness being probably smaller than the coherent XRD domain. As the reaction proceeds, particles grow thicker and more equant. The distribution of I/S particle dimensions forms steady state profiles showing log-normal distribution; however, *sensu stricto* Ostwald ripening is unlikely. It seems that the reaction proceeds toward minimization of the surface free energy of I/S, being affected principally by temperature and K-availability. The spatial distribution of expandability implies that the heating source was probably a mineralized vein with  $T < 200^{\circ}\text{C}$ , directed away from the bentonite, suggesting that illitization might be used as an exploration guide for mineral deposits.

**Key words**—Bentonite, Hydrothermal alteration, Illitization, Illite/smectite, Kaolinite, Neof ormation, Ostwald ripening, Solid state transformation.

## INTRODUCTION

Illitization of smectite has been studied extensively over the past 25 years. The smectite to illite transition is a continuous reaction taking place during burial diagenesis, (Hower *et al* 1976, Boles and Franks 1979, Ramseyer and Boles 1986, Glasmann *et al* 1989), in bentonites (Huff and Türkmenoglu 1981, Altaner *et al* 1984), during contact and burial metamorphism (Nadeau and Reynolds 1981) and during hydrothermal alteration (Inoue and Utada 1983, Harvey and Browne 1991). Illitization has also been observed in atmospheric conditions during wetting and drying cycles (Eberl *et al* 1986) or in saline environments (Singer and Stoffers 1980). Recently, Eberl *et al* (1993) observed low temperature illitization of smectite under alkaline conditions in the laboratory.

The factors which control the reaction are temperature (Hower *et al* 1976, Harvey and Browne 1991), pressure (Velde and Nicot 1986), K-availability (Howard and Roy 1985), pore fluid chemistry (Robertson and Lahann 1981), smectite composition (Eberl *et al* 1978, Boles and Franks 1979), permeability (fluid/rock ratio) and residence time (Ramseyer and Boles 1986, Whitney 1990). The reaction involves release of chem-

ical elements which participate in the formation of quartz, chlorite and/or kaolinite by-products (Hower *et al* 1976). The abundance of chlorite depends on K-availability (Whitney and Northrop 1988) while that of kaolinite depends on the  $\text{K}^+/\text{H}^+$  activity ratio of the fluid.

So far the mechanism of illitization is not understood in detail. The assumption for solid state transformation (Hower *et al* 1976) with partial dissolution of smectite, known as “cannibalization of smectite” (Boles and Franks 1979) was questioned by Nadeau *et al* (1984a, 1984b, 1984c) who presented the neof ormation scenario in their concept of fundamental particles, although Bethke and Altaner (1986) in their attempt to support the McEwan crystallite model, used a Monte Carlo statistical model to show that a layer-by-layer illitization, the solid state transformation assumption, may be valid. Based on a TEM study Inoue *et al* (1987) showed that the transition is a stepwise process involving potassium fixation (solid transformation) for the random interstratified illite-smectite, followed by dissolution and precipitation of ordered illite-smectite (neof ormation). The latter finally gives rise to 2M1 illite in an advanced stage after transformation of illite-rich particles. A different illitization mechanism for

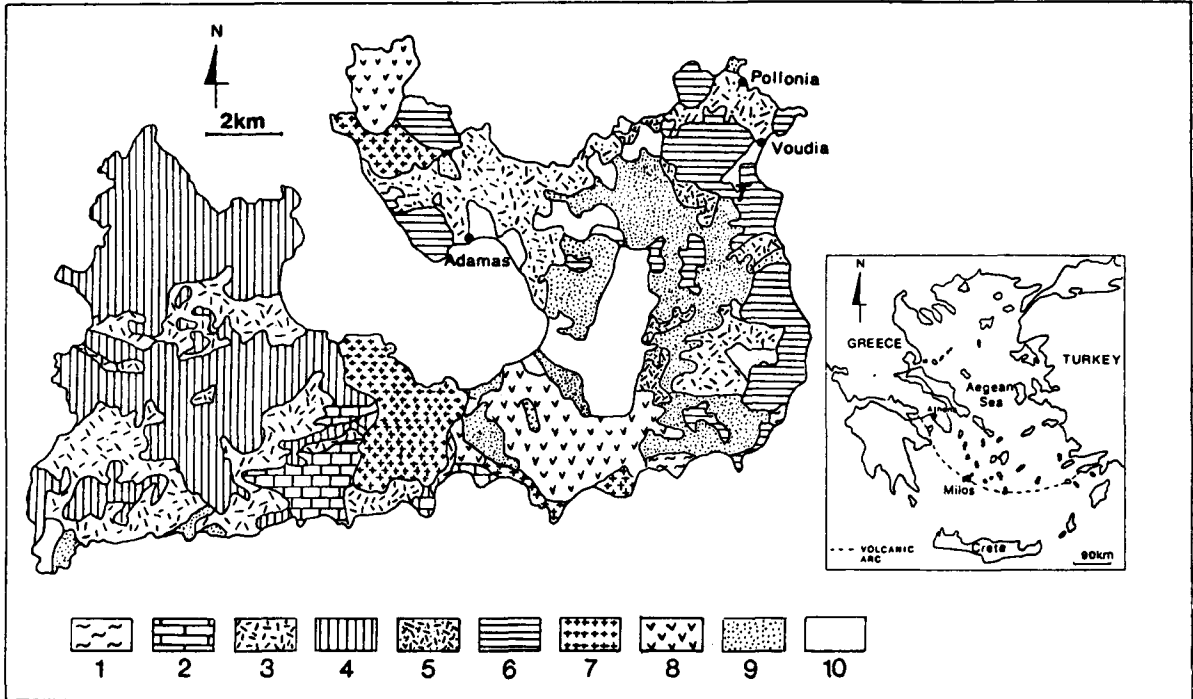


Figure 1. Simplified geological map of Milos Island, modified after Fyticas *et al* (1986). Key to the numbers: 1 = Metamorphic basement, 2 = Neogene Sedimentary Sequence, 3 = basal pyroclastic series, 4 = complex of lava domes and lava flow (Upper Pliocene) 5 = Lower Pleistocene pyroclastics (protoliths of bentonite), 6 = Lower Pleistocene lava domes, 7 = Halepa and Plaka lava domes, 8 = Rhyolitic complexes of Trachilas and Phyrilpaka, 9 = Products of phreatic activity, 10 = Quaternary sediments. T = Tsantilis bentonite deposit.

random and ordered interstratification was also postulated by Whitney and Northrop (1988) in hydrothermal experiments. Based on HRTEM observations, Lindgreen and Hansen (1991) considered illitization of smectite from North Sea sediments might have proceeded via solid state transformation.

Detailed TEM and XRD studies (Eberl and Srodon 1988, Inoue *et al* 1988, Eberl and Sucha *et al* 1990, Sucha *et al* 1993) showed that the growth of illite-smectite particles might be controlled by Ostwald ripening, characterized by dissolution of unstable (subcritical) particles, followed by growth of stable (supercritical) particles (Baronnet 1982, 1984). Lanson and Champion (1991) questioned the application of Ostwald ripening process *sensu stricto* in the diagenetic environment they studied.

In the present study, transmission and scanning electron microscopy (TEM-SEM) techniques in addition to X-ray diffraction (XRD) and X-ray fluorescence (XRF), were used in order a) to examine the morphological changes caused in the clay particles in a smectite-to-illite conversion observed in the hydrothermal field of Milos Island Greece, b) to determine whether the transition is controlled by Ostwald ripening, c) to examine the role of by-products in the evolution of illite-smectite particles, and d) to use the observed al-

teration pattern as an exploration guide for mineral deposits.

## GEOLOGIC SETTING

The volcanic island of Milos is part of the South Aegean Arc, which extends from the Saronic Gulf (Suzaki, Aegina, Poros, and Methana Volcanoes), to the Asia Minor Coast (Nisyros, Kos, Bodrum Volcanoes) passing through the Southern Aegean Volcanic Centers of Milos, Kimolos and Santorini Islands (Figure 1). The volcanic activity was initiated during the Upper Pliocene epoch (Fyticas *et al* 1986) and is still active today in the form of solfatara activity. The geological-volcanological features of Milos Island (Figure 1) have been described by Fyticas *et al* (1986).

A large number of bentonite deposits of Lower Pleistocene age have been formed from the low temperature alteration of glassy pyroclastic rocks in a submarine environment in Eastern Milos (Christidis *et al* 1995). The bentonite deposits have been affected by subsequent hydrothermal alteration, which is still active today in the form of thermal springs, and is related to the geothermal field of the Island. The influence of hydrothermal alteration on bentonites includes decrease of the smectite content via replacement by ka-

olinite and/or halloysite and precipitation of various silica polymorphs, carbonates, sulphates and sulphides as well as illitization of smectite (Christidis 1992). The main terrain in which illitization takes place is the Tsantilis deposit.

The Tsantilis deposit (Figure 1) is a massive bentonite deposit with a thickness greater than 40 m, formed at the expense of a volcanic breccia of andesitic composition and consisting principally of a Wyoming-type montmorillonite and authigenic K-feldspar (Christidis and Dunham 1993, Christidis *et al* 1995). The influence of subsequent hydrothermal alteration is visible macroscopically in the form of gypsum veins, S-metasomatism along fault planes, and formation of mixed layer illite-smectite in the southern sector of the deposit (Christidis 1992).

## MATERIALS AND METHODS

### *X-ray diffraction*

Twenty-five samples were collected from the southern sector of the deposit along vertical and horizontal profiles, 35–40 cm below the surface to minimize the effect of weathering. Bulk mineralogy was determined by X-ray diffraction on randomly oriented air dried samples. Clay mineralogy was determined in samples soaked in distilled water overnight and subsequently dispersed with ultrasonic vibration for 2 minutes using Na-polymetaphosphate. The less than 1  $\mu\text{m}$  size fraction was separated using sedimentation, spread on glass slides and allowed to dry in atmospheric conditions. The dried clay samples were saturated with ethylene-glycol vapor at 60°C for 16 hours and X-rayed immediately with a Philips diffractometer (PW1710 control unit), using at 40 kV and 30 mA, using Ni-filtered  $\text{CuK}\alpha$  radiation. Scanning speed for all samples was 1° 2 $\theta$ /min. Semi-quantitative analysis of the glycolated clay fractions were obtained using the methods of Reynolds (1989). Expandability of illite-smectite (I/S) was determined using the methods of Srodon (1980). The definition of reichweite (R) values used in this paper follows that of Jagodzinski (1949).

### *Electron microscopy*

Broken surfaces of representative samples, covering the whole range of expandabilities, were coated with gold and examined with a Hitachi S520 SEM operating at 20 kV accelerating voltage, equipped with a Link AN1000 Energy Dispersive Spectrometer (EDS) for qualitative analyses. The less than 1  $\mu\text{m}$  of representative clay fractions were dispersed in distilled water (1 mg clay/40 ml of water), spread on freshly cleaved mica surfaces, allowed to dry in atmosphere, shadowed with Pt at an angle of 8°, coated with carbon (Beutelspacher and van der Marel 1968), mounted on copper grids and examined with a JEOL 100CX TEM. Particle size measurements (length, width and aspect ratio) were

Table 1. Mineralogical composition of the original bentonite and the K-bentonite product of illitization in the Tsantilis deposit. Data came from 25 samples. M = major mineral, Min = minor mineral, T = accessory mineral, ( $\pm$ ) = present in places, <sup>1</sup> = authigenic <sup>2</sup> = present in the silicified horizon. (Figure 2), † = secondary, product of hydrothermal alteration.

Minerals present	Original bentonite	K-bentonite
Smectite-type	M (Wyoming-type montmorillonite)	—
K-feldspar <sup>1</sup>	M	M
Illite/smectite	—	M
Kaolinite	T/Min ( $\pm$ )†	T/Min ( $\pm$ )
Quartz	Min ( $\pm$ )†	M <sup>2</sup>
Calcite	Min ( $\pm$ )†	Min ( $\pm$ )
Siderite	Min ( $\pm$ )†	Min ( $\pm$ )
Ankerite	Min/M ( $\pm$ )†	Min/M ( $\pm$ )
Alunite	—	Min ( $\pm$ )
Jarosite	T/Min ( $\pm$ )†	T/Min ( $\pm$ )
Gypsum	T ( $\pm$ )†	T ( $\pm$ )
Pyrite	T ( $\pm$ )†	T ( $\pm$ )

made only on lath-like particles, on a digitizing table, using a computer program of Dr. A. Low (Biology department Univ. of Leicester). Particle thickness was determined on both lath-like and flaky particles by measuring the shadow of each particle, using a 10 $\times$  magnifier with a graticule and converting the measurement to particle thickness. A minimum of 150 particles were measured from each sample. Two aspect ratios (AR) were determined; one refers to the surface of the particle (length : width), and the second the thickness (length : thickness).

### *X-ray fluorescence*

Representative samples were dried at 105°C, ground to pass from a 125  $\mu\text{m}$  sieve and analyzed with X-ray Fluorescence (XRF). Element concentrations were obtained from fusion beads, using a mixture of 80% Li-tetraborate and 20% Li-metaborate as flux (Bennett and Oliver 1976 modified by N. Marsh, University of Leicester). Each sample was analyzed for Si, Ti, Al, Fe, Mn, Mg, Ca, Na, K, S and P. Total iron was expressed as  $\text{Fe}_2\text{O}_3$ . Accuracy and precision of the analysis was tested by means of international standards (Govindaraju 1989). Determination of  $\text{SO}_3$  was carried out using a series of baryte standards with different S-contents in a bentonite matrix.

## RESULTS

### *Mineralogy*

The mineralogical composition of both the original bentonite and the K-bentonite which resulted from illitization is given in Table 1. Mixed layer illite-smectite (I/S) and authigenic K-feldspar are the main constituents of the illitized bentonite. There is no indication for an inverse relationship between the amount of K-feldspar and expandable layers. Minor minerals

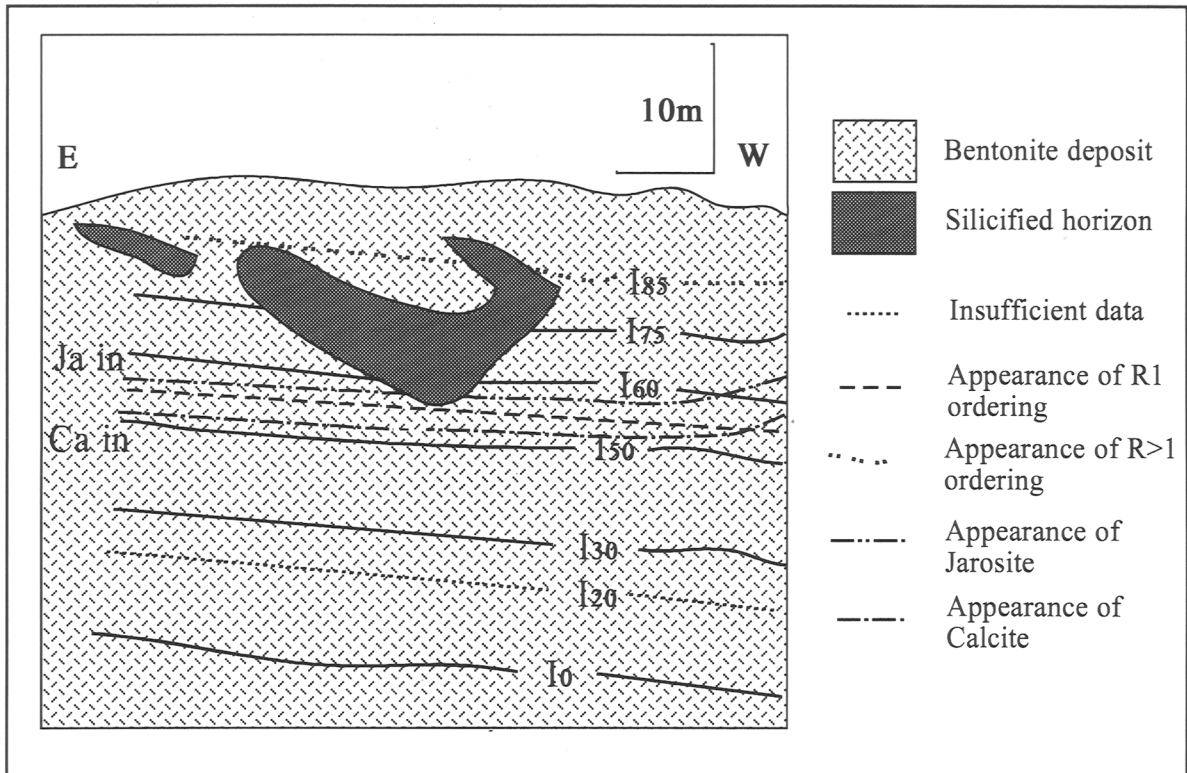


Figure 2. Schematic cross section of the south sector of the Tsantilis deposit.  $I_i$  ( $i = 0-85$ ) is the illite content of the I/S determined using the methods of Srodon (1980). Ca = carbonates and Ja = jarosite.

are kaolinite, carbonates, jarosite and gypsum, while alunite and pyrite are accessory minerals. Quartz was not identified within the K-bentonite, being abundant in the silicified zone at the higher levels of the deposit (Figure 2) and in samples with no indication of illitization. Three types of carbonates were recognized, ankerite, siderite, and calcite, the former being more abundant. In the less than  $1 \mu\text{m}$  clay fractions I/S is the dominant mineral with kaolinite present in amounts varying from 7 to 18% (Figure 3). The kaolinite content does not vary systematically with increasing illitization. Chlorite was absent in both the bulk samples and the clay fractions.

With the exception of gypsum which is dispersed in small amounts throughout the studied area, the distribution of the sulphates and carbonates follows certain trends (Figure 2). Jarosite and alunite occur in the unaltered bentonite and the upper levels of the K-bentonite coexisting always with gypsum but rarely with small amounts of kaolinite and never with carbonates. The carbonates occur in the lower levels of the K-bentonite and the unaltered bentonite and are usually associated with kaolinite. A similar distribution pattern is followed by pyrite.

The amount of illite in the I/S increases toward the

higher stratigraphic levels of the bentonite and from east toward west (Figure 2). Interstratification is random in the lower levels of the deposit becoming ordered ( $R = 1$ ) in the range of 50–43% expandable layers (Figure 3), in agreement with other studies (Inoue and Utada 1983, Brusewitz 1986, Srodon *et al* 1986, Inoue *et al* 1987). Coexistence of both random and ordered interstratification ( $R_0/R_1$ ) was observed in the samples with range 50–45% expandable layers. The  $R_1$  I/S can be classified as fully ordered or partially ( $1/2$  ordered) using the diagrams of Srodon (1980) (Figure 4). The partially ordered I/S are always associated with kaolinite. Finally  $R > 1$  type ordering was observed at expandabilities below 18%. The lowest amount of expandable layers found was 13%.

#### Chemistry

The XRF results are given in Table 2. Illitization is associated with removal of Si, Fe, Mg, Ca and Na and increase of the Al-content in the samples SM82, SM89, and SM94, which is probably of residual character (Christidis 1992). K displays a 5- to 6-fold increase, relative to the original bentonite, indicating that it has been introduced to the system. The  $\text{K}_2\text{O}$  content is unusually high even when the typical K-content of the

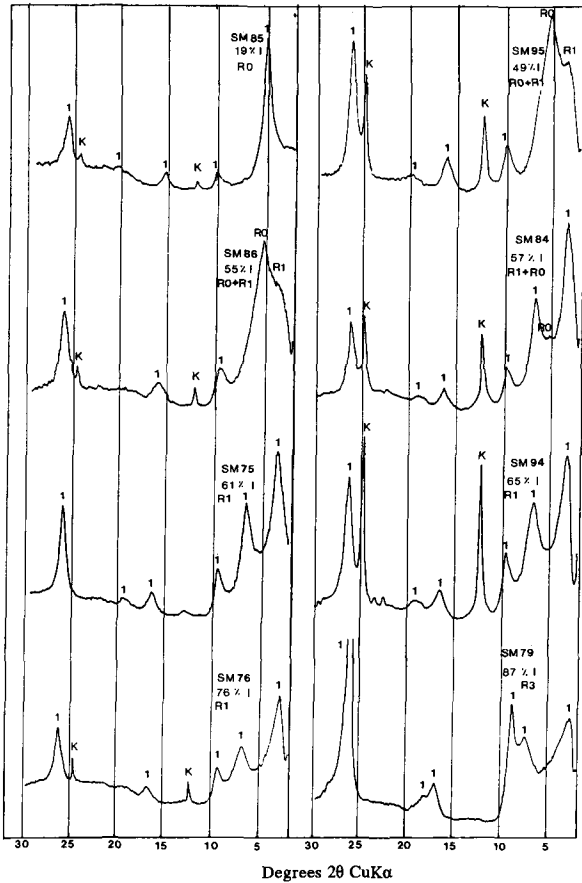


Figure 3. Representative XRD traces of the less than 1 μm clay fractions. 1 = mixed layer I/S, K = kaolinite, I = illite content.

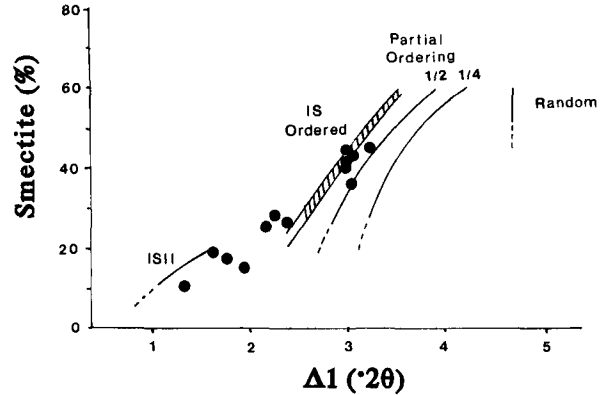


Figure 4. Characterization of the ordering of the illites/smectites according to the methods of Srodon (1980).

end member illite is considered (Newman and Brown 1987). This might probably be due to the presence of exchangeable K in the expandable layers of I/S and/or to the greater amount of authigenic K-feldspar, especially in SM75 and SM78. The almost complete removal of Ca indicates that exchangeable K might be present. Massive K-influx in SM75 and SM78 and Fe-supply in SM78 might explain the constant Al-content, since it has outbalanced the removal of Si, Mg, Ca, Fe and Na.

With the exception of Si (Figure 5), no relationship holds between expandability and either the K-content or the remaining released elements probably due to the presence of other minerals. Thus, the higher Fe-content of SM82 and SM94 might be due to the presence of jarosite, while SM78 contains jarosite and hematite. In SM78 Fe might also be present in the I/S structure,

Table 2. Representative chemical analysis of the original bentonite (SM100) and the K-bentonite (remaining analyses). The kaolinite percentage refers to the clay fraction. The Si/Al fraction is not only an indication of the degree of illitization but reflects also the presence of kaolinite. n.d. = below detection limits, LOI = loss on ignition.

	SM100	SM75	SM78	SM82	SM89	SM94
SiO <sub>2</sub>	58.52	56.77	53.79	51.49	54.43	53.78
TiO <sub>2</sub>	0.90	0.88	0.89	1.09	1.12	1.13
Al <sub>2</sub> O <sub>3</sub>	19.91	19.94	19.64	21.58	23.12	22.54
Fe <sub>2</sub> O <sub>3</sub>	4.05	1.91	5.89	2.36	1.76	2.47
MnO	0.11	0.01	0.10	0.01	n.d.	0.01
MgO	3.34	0.79	1.45	1.06	1.02	1.10
CaO	2.21	0.34	0.25	0.14	0.16	0.14
Na <sub>2</sub> O	0.48	0.37	0.20	0.26	0.35	0.28
K <sub>2</sub> O	1.72	10.10	9.90	8.35	8.38	8.71
P <sub>2</sub> O <sub>5</sub>	0.13	0.09	0.06	0.04	0.05	0.05
LOI	6.69	5.51	6.50	12.57	8.82	8.85
SO <sub>3</sub>	1.69	n.d.	0.50	0.24	0.52	0.45
Total	99.75	99.87	99.12	99.19	99.73	99.51
Expandability (%)	100	40	16	17	47	35
Reichweite (I/S)	—	R1	R > 1	R > 1	R0/R1	R1
Si/Al	2.94	2.85	2.74	2.39	2.35	2.39
Kaolinite (%)	—	—	—	—	17	13.2

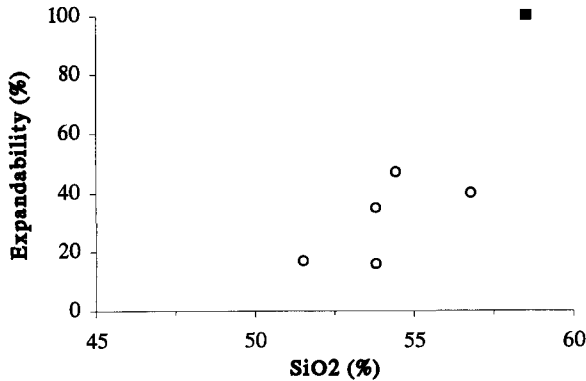


Figure 5. SiO<sub>2</sub> vs expandability in K-bentonite samples from the south sector of the Tsantili deposit. The open square corresponds to the unaltered bentonite.

since its Al-content is low when the illite content is taken into account. Also, jarosite and gypsum contain SO<sub>3</sub> which was detected in most samples. Finally, the relatively higher Al-content of SM89 and SM94 is probably associated with the presence of kaolinite (17% and 13.5% of the clay fraction respectively).

#### I/S morphology—SEM observations

Representative SEM micrographs of the K-bentonite are given in Figure 6. I/S occurs in the form of both flakes and laths. Illitization has caused two main textural modifications on the original smectite flakes: 1) Flattening of the original wavy flakes; and 2) Formation of illite/smectite laths at expandability as high as 75%.

Keller *et al* (1986) reported that illitization proceeds causing flattening of the smectite flakes and subsequent formation of scallops at their edges, in agreement with this work. However, they reported the existence of I/S ribbons only close to the pure illite member (12% smectite). This work showed that lath-like I/S formed at lower expandabilities in good agreement with TEM observations (e.g., Inoue *et al* 1988). Within the limitation of the qualitative analysis it was not possible to observe differences in the chemistry of the flaky and the lath-like I/S. K-feldspar has been replaced by I/S in places (Figure 6) indicating that it might be a limited provider of K.

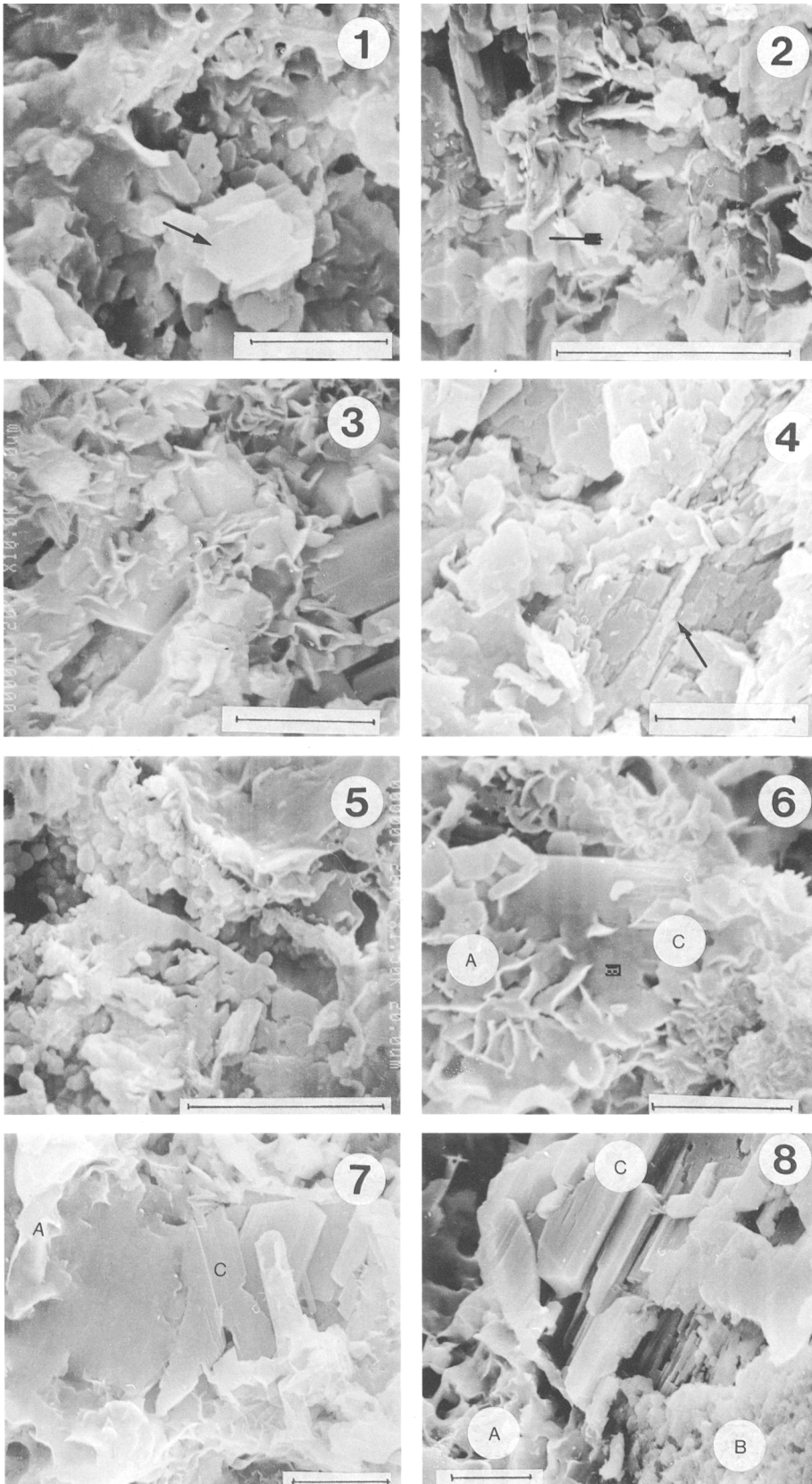
#### TEM observations

**Smectite.** It occurs mainly in the form of subhedral particles (S-type smectite after Güven and Pease 1975) (Figure 7), although lath-like particles with polygonal outlines (L-type smectite) or even euhedral particles (E-type crystals) are also present. The L-shaped smectites have thickness ranging from 30 to 50 Å, while the subhedral ones between 30 and 90 Å. The distribution of thickness in the smectite particles is depicted in Figure 8. The minimum thickness was 30 Å and the average 44.5 Å ± 11.7 Å (Table 3). Single smectite particles 10 Å thick, were not separated in pure smectitic materials in accordance with Güven (1974) and Güven and Pease (1975), but contrary to Mering and Oberlin (1971) and Nadeau *et al* (1984a, 1984b). This difference might be attributed to different sample preparation methods, since in this work the samples were not saturated with sodium (Güven and Pease 1975). It is interesting that 10 Å particles were isolated in randomly interstratified I/S using similar separation techniques.

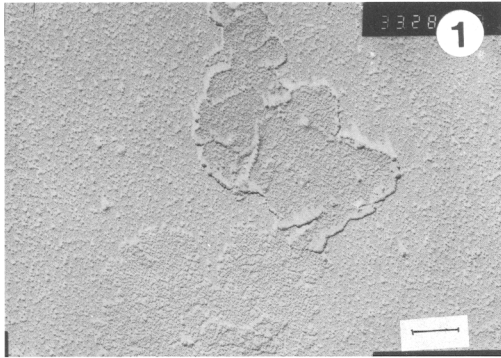
**Illite/smectite.** It occurs in the form of both laths and flakes (Figure 7). In places lath-like particles display edge-to-edge association forming larger flakes. The abundance of laths increases with decreasing expandability. An exception to this trend is shown by the sample SM84 in which I/S displays ordered R1-type interstratification with 44% expandable layers but is dominated by flaky particles. Due to the limited number of lath-like particles in this sample, statistical analysis of length and width measurements were not performed. Such an existence of flaky I/S crystals seems to contradict the suggestion of Inoue *et al* (1987, 1988) about the relationship between lath-shaped and flaky I/S particles. SM84 contains abundant kaolinite (12%) in the clay fraction.

The results from statistical analyses of length, width, thickness and aspect ratios (length : width and length : thickness ratio) of I/S particles of different expandabilities are listed on Table 3. The change of each dimension with decreasing expandability is depicted in Figure 9, while the histograms of thickness are shown in Figure 8. It is obvious that the total number of thickness measurements can be subdivided into distinct populations with mean thickness multiples of ca.

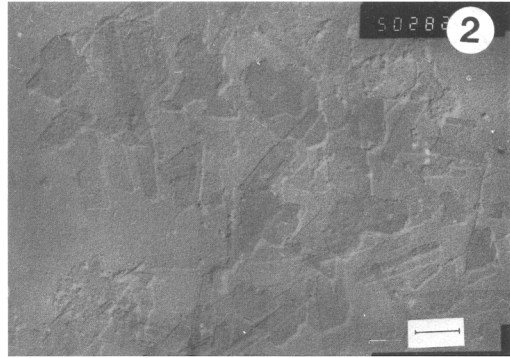
Figure 6. SEM micrographs of the illite/smectite in the southern sector of the Tsantili deposit. 1, 2. Kaolinite (shown with arrow) associated with illite/smectite. Kaolinite was probably formed as a by-product during illitization. Scale bars 1 = 4.3 μm, 2 = 2.5 μm. 3. Illite/smectite forming at the expense of euhedral crystals of authigenic K-feldspar. Scale bar 4.3 μm. 4 = Small illite/smectite laths (shown with arrow) coexisting with flat flakes, which are also illite/smectite. The I/S is characterized by random interstratification. (75% expandability). Scale bar 4.3 μm. 5. Coexistence of illite/smectite laths and flakes at 26% expandability. Ordered (R1) interstratification. Scale bar 3 μm. 6. Coexistence of flaky (A) and lath-like (C) I/S crystallites. 6 = 17% expandability, (R > 1), 7 = 13% expandability (R > 1). Scale bars: 6 = 4.3 μm, 7 = 6 μm. 8. Coexistence of flaky (A and B) and lath-shaped (C) illite/smectite crystallites. Two types of I/S flakes are present: well formed wavy flakes (A) and small flakes (B). Both types seem to evolve to the lath shape crystallites (C). Expandability 13% (R > 1). Scale bar 7.5 μm.



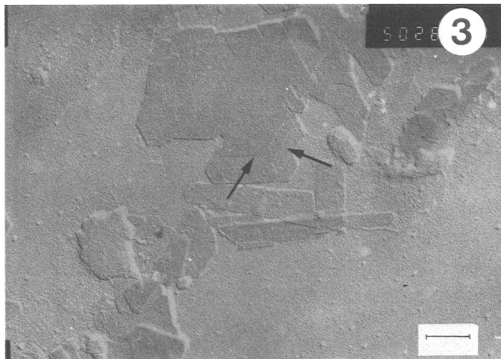
100% S



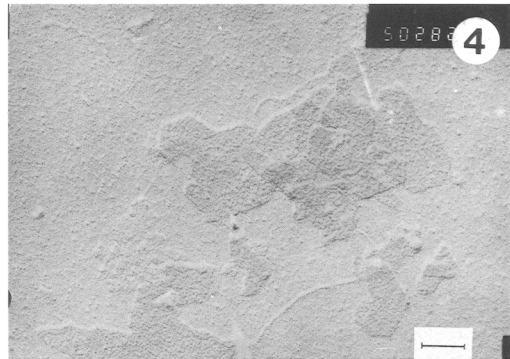
74% S



51% S



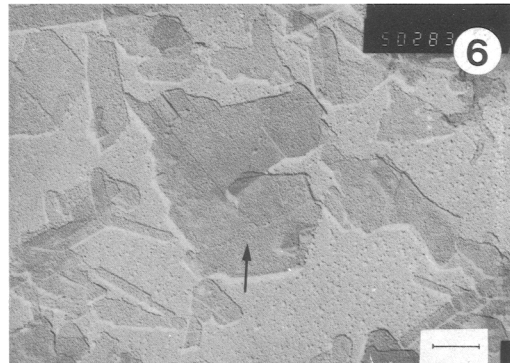
44% S



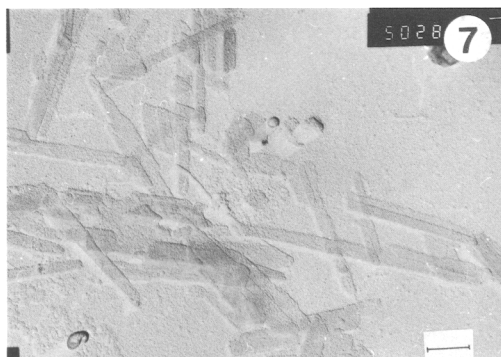
40% S



35% S



24% S



13% S

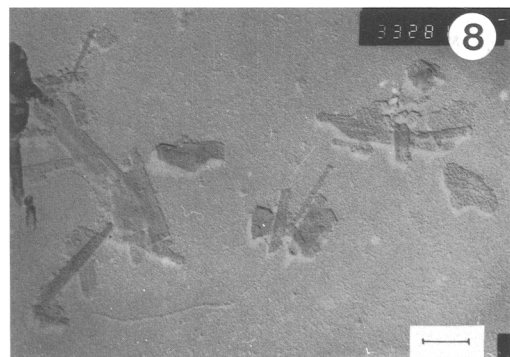


Table 3. Size (length, width and thickness) measurements of the illite/smectite particles present in the Tsantilis deposit, Milos. Length and width are in micrometers and thickness in nanometers. Aspect ratio is the length : width and aspect ratio† is the ratio length : thickness. Expandability refers to the percentage of smectite layers present in the I/S according to the methods of Srodon (1980).

	SM85	SM91	SM95	SM86	SM75	SM94	SM76	SM82	SM78	SM79
Expandability (%)	81	74	51	45	40	35	24	17	16	13
Mean Length	0.27	0.28	0.30	0.34	0.36	0.27	0.29	0.26	0.26	0.28
Std. Deviation	0.11	0.12	0.16	0.14	0.15	0.12	0.15	0.11	-/13	0.13
Min. Length	0.09	0.07	0.08	0.12	0.09	0.03	0.07	0.09	0.07	0.07
Max. Length	0.65	0.77	1.41	0.90	0.88	0.70	1.04	0.87	0.82	0.81
Mean Width	0.04	0.04	0.04	0.04	0.05	0.04	0.04	0.05	0.05	0.06
Std. Deviation	0.01	0.01	0.02	0.01	0.02	0.01	0.02	0.02	0.01	0.02
Min. Width	0.02	0.01	0.02	0.03	0.02	0.01	0.01	0.02	0.01	0.02
Max. Width	0.09	0.10	0.10	0.09	0.12	0.07	0.19	0.13	0.08	0.20
Mean Aspect Ratio	6.75	7.00	7.50	7.60	7.20	6.75	7.25	5.20	5.20	4.70
Mean Aspect Ratio†	150	155.56	157.89	141.67	133.33	100	93.55	68.42	81.25	68.29
Mean Thickness	1.80	2.40	1.90	2.40	2.70	2.70	3.10	3.80	3.20	4.10
Std. Deviation	1.70	0.44	0.40	0.44	0.89	0.61	0.93	0.99	0.83	1.20
Min. Thickness	0.80	1.30	1.20	1.30	1.40	1.40	1.70	2.20	1.80	1.20
Max. Thickness	3.50	3.90	2.90	3.90	6.20	4.70	6.70	7.80	5.80	8.50
Particle No.	159	183	126	183	142	170	228	214	157	208

10 A. The slight deviation from exact multiples of 10 A might be due either to the precision of the experimental method ( $\pm 4-5$  A) or to stacking faults in the particles. It is observed that with decreasing expandability (Figures 9 and 10):

(1) The minimum and mean thickness of the I/S particles increases.

(2) The abundance of 10 A thick particles decreases steadily. They disappear completely at about 50% expandable layers when interstratification becomes ordered.

(3) The abundance of 20 A thick particles increases steadily up to the point where the character of interstratification changes from random to ordered and then decreases almost linearly. Extrapolation to 0% 20 A particles gives 12% expandability. It is clear that the I/S with random interstratification is composed of 10 A and 20 A thick particles, the relative proportion of which changes reversibly with expandability, in accordance to Nadeau *et al* (1984c).

(4) The 30 A thick I/S particles appear at 45% ex-

pandable layers. Due to the lack of 30 A thick particles in I/S with R0, their existence in SM86 which is characterized by both random and ordered interstratification must be connected with the ordered I/S layers. Their abundance is nearly constant down to 25% expandable layers, decreasing thereafter.

(5) The 40 A thick I/S particles appear at 45% expandable layers, increasing steadily up to about 25% expandable layers and then exhibit a sharp decrease.

(6) The population of the 50 A particles is constant down to 25% expandable layers and then increases suddenly, becoming the dominant particle thickness of the I/S with  $R > 1$ .

(7) The 60 A particles are absent at expandabilities higher than 25% increasing steadily thereafter.

The mean length of the lath-like particles increases steadily up to 50% expandability and then decreases steadily. The maximum mean length coincides with the appearance of R1 ordering. The mean width remains virtually constant until about 20% expandability and then increases rapidly, in accordance with Inoue

←

Figure 7. TEM micrographs of Pt-shadowed less than 1  $\mu\text{m}$  clay fractions of smectite (original bentonite) and illite/smectite (K-bentonite). 1 = S-type (subhedral) smectite flakes (100% expandability). Scale bar 0.25  $\mu\text{m}$ . 2 = Lath-like particles coexisting with flakes. The former are predominately 20 A thick. 74% expandability (R0). Scale bar 0.15  $\mu\text{m}$ . 3 = Step-like growth (shown with the arrow) of illite/smectite particles, forming a large flake. The I/S laths are oriented nearly parallel to the direction of shadowing, towards the upper part of the photograph, and show both edge-to-edge and edge-to-face association. 51% expandability (R0/R1). Scale bar 0.15  $\mu\text{m}$ . 4. Predominance of flaky crystals at 44% expandable layers. The thickness of the flakes is 20 A and 30 A. R1/R0 ordering. Scale bar 0.15  $\mu\text{m}$ . 5 = Predominance of illite/smectite lath-like particles at 40% expandability (R1). Scale bar 0.15  $\mu\text{m}$ . 6 = Possible step-like growth (shown with the arrow) at 35% expandable layers. The particles show both face-to-face and edge-to-edge association. The large "flake" in the center consists of several lath-like particles. R1 ordering. Scale bar 0.15  $\mu\text{m}$ . 7 = Illite/smectite laths at 24% expandable layers. Flaky crystallites are absent. R1 ordering. Scale bar 0.15  $\mu\text{m}$ . 8 = Illite/smectite laths at 13% expandable layers. ( $R > 1$ ). The particles show face-to-face association. Scale bar 0.25  $\mu\text{m}$ .

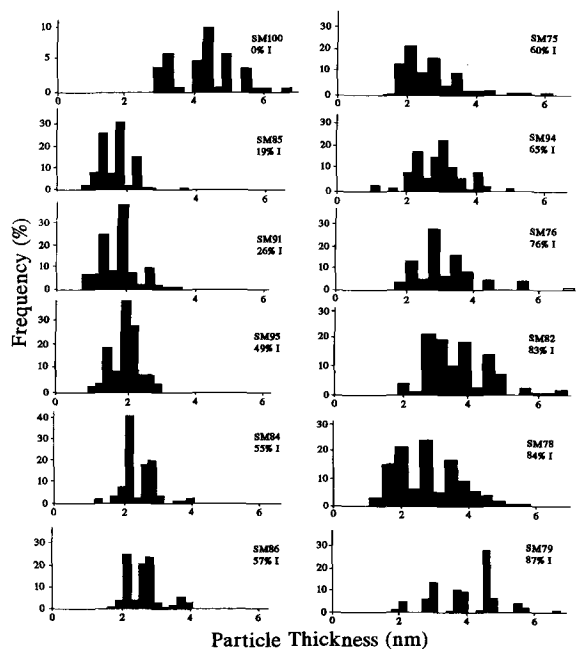


Figure 8. Histograms showing the distribution of thickness of smectite and illite smectite particles. Note the maxima at multiples of 10 Å. The minimum thickness of the smectite particles (unaltered bentonite) is 30 Å.

*et al* (1988). It follows that as illitization proceeds the illite/smectite particles become more equant. The hexagonal illite crystals observed by Inoue *et al* (1988) and Lanson and Champion (1991) close to the illite end (growth transformation of Inoue *et al* 1987) were not observed.

The results obtained from measurement of the length, width and thickness of the I/S particles of different expandabilities were plotted in histograms with reduced coordinates ( $r/r_{av}$  vs.  $f(r)/f(r)_{max}$ ). The profiles obtained (Figure 11) display steady state distribution *ie* independent of the mean particle size and the initial particle size distribution of the clay particles, constituting indirect evidence for growth of the particles via Ostwald-ripening (Lifshitz and Slyozov 1961, Baronnet 1982, 1984). These steady state profiles have maxima in the same area ( $r/r_{av}$  is 0.9–1) and are comparable to those presented by other workers (Inoue *et al* 1988, Eberl and Srodon 1988, Eberl *et al* 1990, Jahren 1991, Lanson and Champion 1991). Each profile obtained is composed of particles formed at different temperatures. Thus, the original relative order of particle sizes did not change, although both the absolute and the relative sizes of the particles changed (Chai 1974). Although they resemble the profiles obtained in hydrothermal experiments for second order kinetics (Baronnet 1982, 1984) they do not seem to fit exactly with any of the theoretical profiles for first order kinetics,

bulk diffusion or second order kinetics. Instead they display log-normal distribution (Eberl *et al* 1990).

Second order kinetics imply low supersaturation conditions and growth by a screw dislocation mechanism (Baronnet 1982, 1984). On the other hand the growth mechanism which caused the log-normal distribution has not been understood so far (Eberl *et al* 1990). In Figure 8 (Photo 3) I/S particles seem to grow via spiral growth controlled by screw dislocation. Each step is about 10 Å thick. This indicates that second order kinetics might explain to some degree the illitization process in the Tsantilis deposit.

## DISCUSSION

### *Factors which affected illitization*

**Temperature.** Hydrothermal alteration suggests that temperature has played a major role in illitization. The conversion of the fully expandable phase to mixed layer I/S with only 13% expandable layers has taken place within less than 40 m, indicating that the temperature profile might have changed dramatically within a small distance.

Comparison with similar studies provides indications about the temperature in the various steps of illitization. In hydrothermal systems the appearance of R1 ordering has been reported at 98–135°C in the Salton Sea hydrothermal system (Muffler and White 1969) and at 85–110°C in the Wairakei hydrothermal system (Srodon and Eberl 1984, Harvey and Browne 1991). The appearance of illite with less than 5% expandable layers has been reported at 200°C in the Shinzan area (Inoue and Utada 1983), at 203–217°C in the Salton Sea system (Muffler and White 1969), and at 230–240°C in Wairakei (Srodon and Eberl 1984). Harvey and Browne (1991) reported illite formation at 200°C and formation of I/S with 80–90% illite layers at 155–190°C in the Wairakei hydrothermal field. Since in Milos, illitization did not proceed to less than 13% expandable layers, the alteration temperature was probably lower than 200°C. Also, R1 I/S might have formed at about 100–110°C.

**K-availability.** The 5- to 6-fold enrichment of K in the K-bentonite, relative to its unaltered counterpart (Table 2), indicates that illitization was the result of K-metasomatism. Had the reaction proceeded mainly with K from the dissolution of authigenic K-feldspar, substantial increase of the K-content would not have occurred. The influence of K-availability can be assessed if SM94 (35% expandable layers and abundant kaolinite) and SM75 (40% expandable layers kaolinite-free), are compared. Although the former has lower expandability its K-content is 1.5% lower. This suggests that although the temperature and K-abundance were probably sufficient to convert smectite into I/S

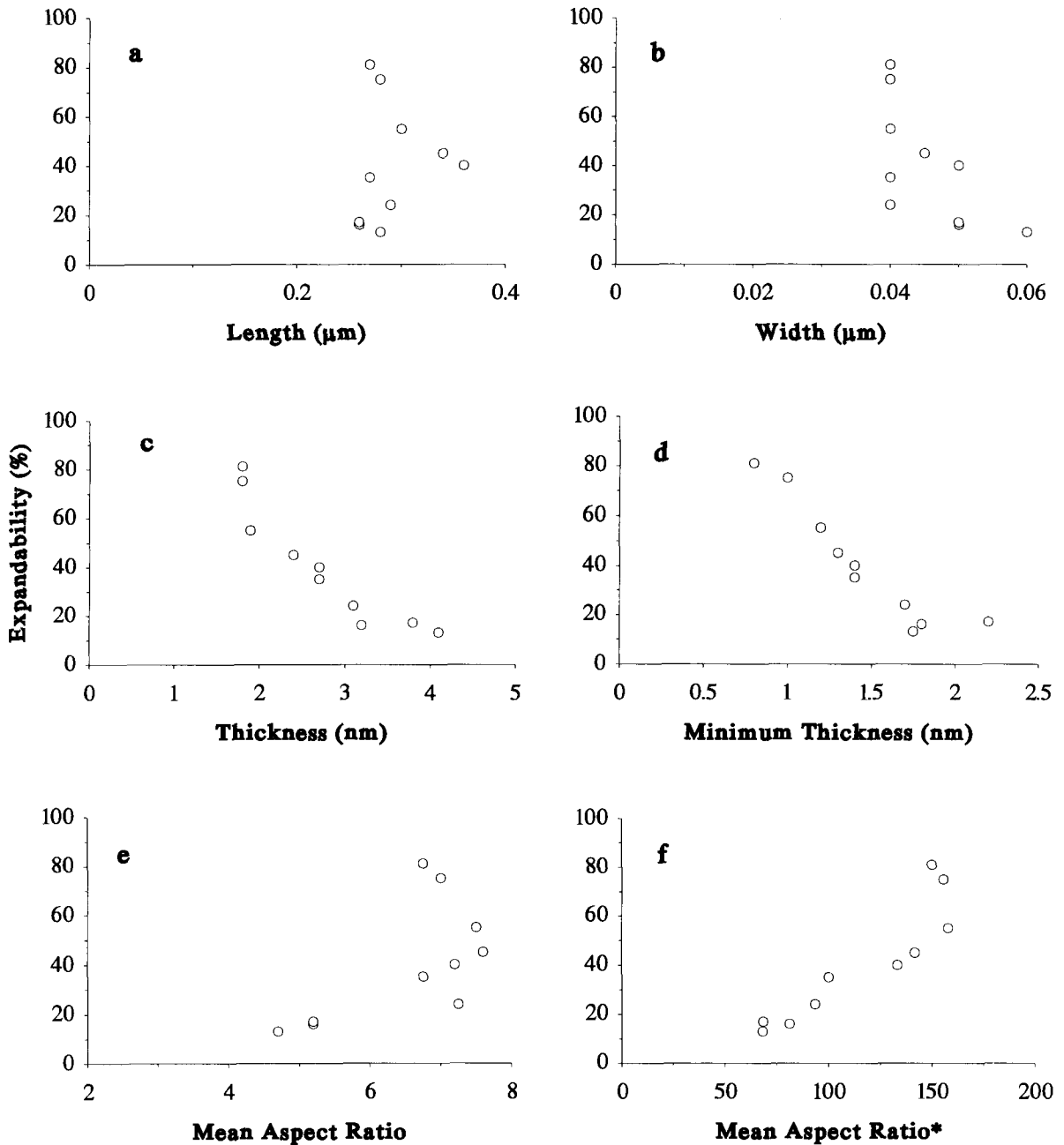


Figure 9. Evolution of the dimensions of the illite/smectite particles with decreasing expandability. The minimum thickness increases with increasing illite content.

with 35% expandable layers, the  $\text{K}^+/\text{H}^+$  activity ratio was low to produce only I/S.

*Pore chemistry.* According to Robertson and Lahann (1981), the presence of  $\text{Ca}^{+2}$  and  $\text{Mg}^{+2}$  in the pore fluids inhibits the reaction rate by an order of magnitude compared with  $\text{Na}^+$ , at a fixed  $\text{K}^+$ -content. However Huang *et al* (1993) found that Ca affects illitization

only barely, Na has significant influence only at very high concentration and only Mg retards the reaction. If it is assumed that the pore chemistry played a major role in the reaction then a geochemical gradient should be expected, characterized by an excess of Mg in the pore fluid in the lower sectors of the deposit and a deficiency in the higher sectors. However, there is no evidence for such a gradient.

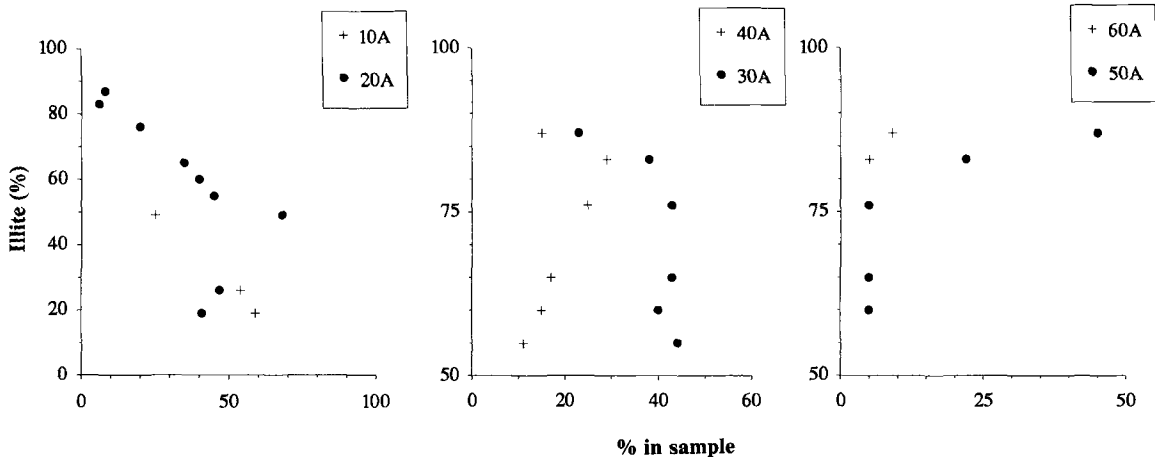


Figure 10. Evolution of the abundance of the illite/smectite particles having various thicknesses, with decreasing expandability.

**Smectite composition.** The Tsantilis deposit contains Wyoming-type montmorillonite with remarkable compositional variation (Christidis and Dunham 1993). Since no systematic zonation in the smectite chemistry has been observed it follows that the role of variation of the smectite chemistry might be rather limited.

**Permeability and residence time.** Permeability is an important factor for illitization, because it provides access to the hydrothermal fluids and determines the nature of the products (Whitney 1990). In this study the by-products observed were either quartz or kaolinite + quartz. Quartz is not present in samples containing I/S, occurring mainly in the silicified zone (Figure 2). High fluid : rock ratios are expected because (1) the emplacement and alteration of the parent rock took place in a marine environment and little or no compaction has taken place and (2) large amounts of K have been transported in the system through fluid flow. There is no reason to suggest that the time in which the materials in the various sectors of the deposit were subjected to hydrothermal alteration was different. Therefore, residence time was probably not important for the observed trends in the composition of illite smectite.

It is believed that the factors controlling illitization in the Tsantilis deposit were temperature and K-availability, which is closely associated with permeability because the K-source was the hydrothermal fluid (K-metasomatism). The presence of samples with a similar K-content but significantly different expandabilities (e.g., SM75 and SM78) suggests that although these samples experienced similar K-influx and water : rock ratios, temperature played the most important role in the reaction. Some of the K consumed might have been supplied by the dissolution of K-feldspar (Figure 6). The Al necessary for the reaction might have

been supplied mainly by the dissolution of smectite ("cannibalization" of smectite after Boles and Franks 1979) and to a much lesser degree by the dissolution of K-feldspar.

#### *Possible mechanism of illitization*

The steady state profiles (Figure 11) indicate that Ostwald ripening might control the growth of I/S. The factors controlling Ostwald ripening have been determined for hydrothermal experiments. The system studied is chemically open (K-metasomatism via hydrothermal solutions). The sense of alteration through fluid flow itself dictates an open system, because the flow path changes continuously with time (Steeffel and van Cappellen 1990). The chemical components released from the dissolution of smectite might have been transported, affecting supersaturation in both the area of dissolution and the area of deposition. Also, potassium might not have been supplied to the same degree in the different sectors of the parent rock. These suggest that the microenvironmental conditions might be important for the smectite to illite transition.

Moreover, the system is not monomineralic. Except for the dissolving smectite, K-feldspar might affect K-availability on a local scale. The formation of kaolinite probably affects smectite dissolution, and possibly the crystal growth and recrystallization of the neofomed illite particles. It also indicates that the mass transfer might not take place only to the neofomed illite particles but to kaolinite as well. Furthermore, other chemical constituents like S and/or  $\text{CO}_3^{2-}$  might have been introduced in the system, affecting the crystallization rate of the I/S (Baronnet 1984). They might also compete with other chemical components derived from the dissolution of smectite, affecting the reaction rate. Finally, it is not known whether there was con-

tinuous or periodic K-supply in the system. Since the K-transport is associated with hydrothermal activity, thus with temperature, the latter might have been constant or might have been varied. Fluctuations in temperature might affect Ostwald ripening (Baronnet 1982).

Although discrepancies from the ideal Ostwald ripening mechanism are observed, illitization was characterized by dissolution of the smaller particles and growth of the larger ones. The particles evolve toward a larger, more equant shape. Thus, even if Ostwald ripening cannot be applied directly, the reaction is directed toward minimization of the surface free energy.

In the incipient stages of illitization (R0 I/S), the changes were probably not significant and were dominated rather by potassium fixation and development of higher layer charge. Lath-like I/S particles were first observed at 80% expandability. (Figure 8). Since the particle morphology is dominated by flaky crystals similar to the smectite ones, the reaction might have involved only limited dissolution of the original flakes. Solid state transformation might have been the dominant mechanism, although the most unstable flakes which had fixed potassium dissolved, and laths 20 Å thick were formed (neof ormation) (Inoue *et al* 1987). In more advanced stages (>50% expandable layers) unstable flakes dissolved and I/S laths formed via neoformation. The first particles to form were 20 Å thick and with advanced illitization, the thickness increased. The newly formed particles became increasingly more isometric in shape.

The variation of the thickness of I/S particles allows for a prediction of possible schematic recrystallization paths during illitization. Thus the fact that the 10 Å particles disappeared at 50% expandable layers, indicates that they might have contributed only to the formation of 20 Å I/S particles and probably did not participate in the formation of 30- and 40 Å thick I/S particles. Also the 30 Å particles seem to have attained a nearly steady state in the range 45–25% expandable layers (Figure 10). It seems that for each particle formed one particle dissolved to form a 40 Å and to a lesser degree a 50 Å thick particle. These 50 Å thick particles might have formed from dissolution of 20 Å particles.

It is not certain if *pure* illite particles, without swelling surfaces, formed during alteration. This study showed that all particles with thickness smaller than 50 Å eventually dissolved during recrystallization with progressing alteration. Since the pure illite particles are the thermodynamically stable end-products of illitization, it follows that in the case studied, their thickness should be >50 Å in accordance with Nadaeu *et al* (1984c). Hence pure illite particles began to form at 40% expandable layers, at a temperature not considerably higher than 100–110°C, and became abundant at expandabilities lower than 25%.

The reaction proposed for illitization might be described by the following dual mechanism:

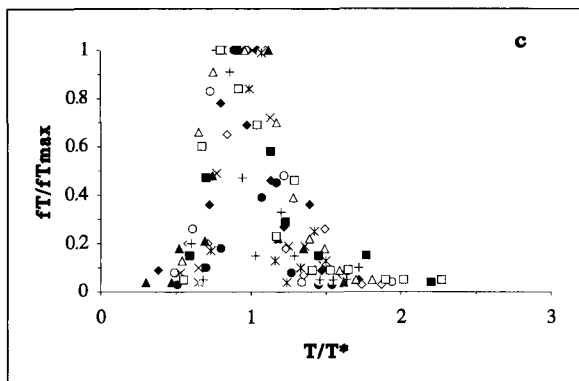
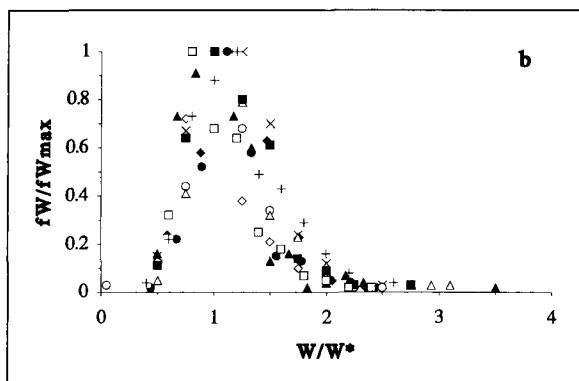
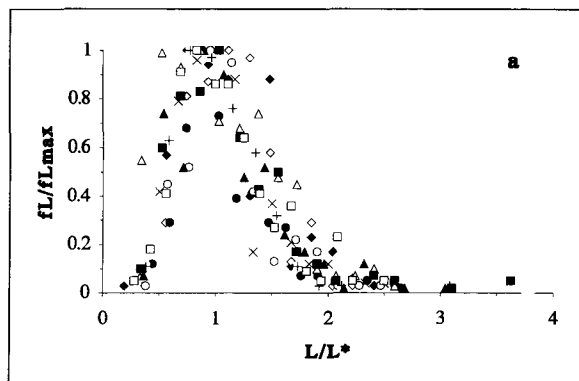
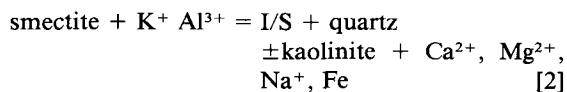
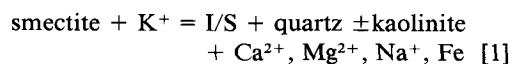


Figure 11. Steady state profiles obtained from (a) length, (b) width, and (c) thickness measurements of the illite/smectite particles. None of the profiles fit any of the experimentally derived profiles (Baronnet 1984).



In reaction [2] K and Al were provided from the dissolution of K-feldspar. Both reactions might pro-

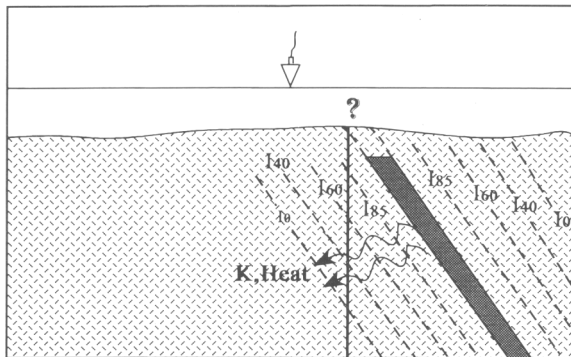


Figure 12. Simplified model proposed for the illitization of the Wyoming-type montmorillonite in the Tsantili deposit. Alteration took place in shallow submarine conditions, but it is not certain if the mineralized vein(s) was discharged on the sea floor (question mark in the extension of the vein). The vertical line represents the cross section in Figure 2.

ceed simultaneously, although the first is of primary importance. The Ca, Na, Mg and Fe released from the reactions [1] and [2] might provide the "nutrients" for the precipitation of gypsum and carbonates, similar to sedimentary sequences (Boles and Franks 1979).

Carbonates are incompatible with jarosite which dictates acidic-oxidizing conditions. Also, the removal of Fe from bentonites during illitization indicates the presence of ferrous iron and implies that alteration took place under reducing conditions. The fact that pyrite is absent from the jarosite bearing-bentonite indicates that it has been replaced by jarosite, suggesting that the character of the hydrothermal alteration is complicated and might have changed with time. Strongly acidic-oxidizing conditions are observed in solfatara springs still active today. Solfatara activity is connected with the formation of kaolin deposits in Milos (Christidis and Marcopoulos 1993). It is believed that the formation of jarosite might not be associated with illitization but might be a later event, which is probably associated with solfatara activity. Similarly, alunite might have been formed at the expense of kaolinite during the same event.

The fact that the intensity of alteration decreases upsection suggests that the heating source was dipping away from the deposit. A possible geological formation which might supply heat and have such geometric characteristics is a mineralized vein containing either ore minerals or barites or might be part of a "barren" thermal conduit (Figure 12). An indication for the possible nature of the vein is provided from the Agrilies bentonite deposit located next to the Pikridou barites deposit. Kalogeropoulos and Mitropoulos (1983) showed that the temperature of the barite veins was between 140 and 170°C. Since the I/S in Agrilies exhibits both random and ordered interstratification (Christidis 1992) it follows that the emplacement of

barite provides a plausible explanation for the heat source, considering its distance from the deposit. This might be the case also for the Tsantilis deposit. Liakopoulos (1987) reported intense K-metasomatism associated with the Ba-Mn mineralization at cape Vani (NW Milos) in support to this view. If the temperature inferred by Kalogeropoulos and Mitropoulos (1983) is valid, the barite body should be very close to the K-bentonite, because the lowest expandabilities observed are expected at temperatures ranging between 150–180°C (Harvey and Browne 1991). Thus illitization of bentonites in Milos might be used as a guide for exploration of barite deposits.

#### *Possible role of by-product kaolinite in illitization*

Kaolinite bearing samples (eg SM84, and SM94) contain abundant flaky I/S particles with thickness up to 30 Å (Figure 8) and partial ordering (Figure 4). Flaky I/S particles with I/S ordering have been reported by Rosenberg *et al* (1990). The existence of flaky I/S particles implies possible formation of I/S via solid state transformation. This association between I/S morphology and kaolinite suggests that dissolution of the unstable flaky I/S particles and formation of lath-like I/S particles might have been retarded by the formation of kaolinite. The mechanism of this reaction scheme might consist of three steps:

- (1) At first unstable smectite flakes and I/S lath-like particles dissolve. All elements released from dissolution are transferred to the pore fluid.
- (2) Then kaolinite precipitates consuming some of the Al and Si released in the pore fluid (neof ormation process).
- (3) Finally I/S forms both by solid state transformation and neof ormation, using the K supplied by the hydrothermal solution, and the dissolution of K-feldspar and the unstable I/S laths. The relative importance of the two processes might depend on the  $K^+/H^+$  activity ratio of the hydrothermal fluid which controls the formation of kaolinite. If the  $K^+/H^+$  activity ratio of the fluid phase is low, probably due to low K-availability or/and to low pH, kaolinite instead of I/S is favored consuming Al and Si released from the dissolution of the unstable smectite and I/S particles. In this case, since K is available, the formation of more illitic I/S particles might proceed mainly through solid state transformation. Thus, kaolinite might counteract the neof ormation of I/S, and contributes to the discrepancy from the ideal Ostwald ripening.

#### *Significance of the TEM observations*

The combination of TEM observation and XRD showed that samples with different particle thickness distribution have similar XRD patterns. Therefore the

coherent domain is probably thicker than the I/S particle (fundamental particle). This is supported by the fact that the sample preparation method used for TEM observation involved dilution of the clay samples in extremely high water : clay ratios. However, even these conditions did not cause dissociation of the smectite quasicrystals to 10 Å smectite particles. The clay suspensions used for separation of the clay fractions in the routine XRD analysis are far more concentrated. Thus it is unlikely to obtain free *sensu stricto* smectite fundamental particles (Nadeau *et al* 1984c) in these suspensions. Similar observations were made for XRD suspensions containing I/S particles.

Ahn and Buseck (1990) published HRTEM micrographs in which I/S with 30% expandable layers and R1 ordering consisted of layer stacks 20- to 50 Å thick, while Veblen *et al* (1990) showed the existence of 2 to 7 illite fringes separated by smectite ones in a sample with 18% expandable layers and  $R > 1$ . These images are comparable with the results of this study for I/S with similar expandability. If we accept the concept of disaggregation of larger coherent units in water along smectite surfaces, which will constitute the edges of fundamental particles of Nadeau and his coworkers, then there is no reason to consider that the original units might necessarily be crystals or the crystallites (due to their size) of Veblen *et al* (1990). Instead, the I/S particles observed in this study (Figure 7), which are comparable to those of Veblen *et al* (1990) and Ahn and Buseck (1990), might constitute the fundamental units of clayey rocks, which might build up thicker units. The author agrees with Veblen *et al* (1990). If the term fundamental particles of Nadeau and his coworkers is used, it should include particles that are not free. HRTEM studies of clay rocks show that the I/S particles form stacks of layers longer than those described in this study. However it is not certain whether these particles are isolated units or form larger ones or the nature of these units. Thus, although Veblen *et al* (1990) showed that in I/S with R1 and  $R > 1$  ordering the coherently stacked layers exceed in thickness the fundamental particles, their cross fringes seem to comprise layers intersecting each other at various angles. It is certain that more detailed work is needed to clarify this point.

### CONCLUSIONS

The Tsantili bentonite deposit in Milos Island Greece has been affected by hydrothermal alteration which converted the original Wyoming-type montmorillonite to illite/smectite with up to 13% expandable layers + quartz ± kaolinite. The alteration profile is characterized by a massive introduction of K and removal of Si, Na, Ca, Mg and Fe from the rock and displays an unusual decrease of the illite content of the I/S with depth. The main parameters controlling illitization are

temperature, K-availability and fluid : rock ratio. The hydrothermal alteration is probably associated with the emplacement of barites veins with temperature lower than 200°C in the close vicinity of the parent bentonite.

The reaction proceeds toward minimization of the surface free energy of the I/S particles which become progressively thicker and more equant. Although the size distribution of all three dimensions of the I/S particles forms steady state profiles showing log-normal distribution, *sensu stricto* Ostwald ripening is unlikely due to the characteristics of the alteration. The formation of kaolinite seems to have retarded neoformation of the I/S particles which form via solid state transformation. With increasing illitization only particles thicker than 50 Å grow, indicating that only these particles are the stable products of the reaction. However it is not certain if they correspond to true illite particles.

### ACKNOWLEDGMENTS

I am indebted to Dr. A. Low and Mrs. E. Roberts of the Biology department, Univ. of Leicester, U.K. for their help and support during the TEM work. The valuable discussions with Prof. A.C. Dunham, D.J. Merriman and the constructive reviews of Drs S.P. Altaner, R.W. Lahann and the editor improved the text. The research was financed by the Greek State Scholarship Foundation (SSF). I am grateful to the Silver and Barytes Ore Mining Co., Greece for their permission to collect samples from bentonite quarries.

### REFERENCES

- Ahn, J. H., and P. R. Buseck. 1990. Layer-stacking sequences and structural disorder in mixed-layer illite/smectite: Image simulations and HRTEM imaging. *Am. Miner.* **75**: 267-275.
- Altaner, S. P., J. Hower, G. Whitney, and J. L. Aronson. 1984. Model for K-bentonite formation: Evidence from zoned K-bentonites in the disturbed belt, Montana. *Geology* **12**: 412-415.
- Baronnet, A. 1982. Ostwald ripening in solution. The case of calcite and mica. *Stud. Geol.* **38**: 185-198.
- Baronnet, A. 1984. Growth kinetics of the silicates. A review of the basic concepts. *Fortschr. Miner.* **62**: 187-232.
- Bennett, H., and G. J. Oliver. 1976. Development of fluxes for the analysis of ceramic materials by X-ray Spectrometry. *Analyst.* **101**: 803-807.
- Bethke, G. M., and S. P. Altaner. 1986. Layer by layer mechanism of smectite illitization and application to a new rate law. *Clays & Clay Miner.* **34**: 136-145.
- Beutelspacher, H., and H. W. van der Marel. 1968. *Atlas of Electron Microscopy of Clay Minerals and Their Admixtures*. Amsterdam: Elsevier, 333 pp.
- Boles, J. R., and S. G. Franks. 1979. Clay diagenesis in Wilcox Sandstones of Southwest Texas: Implications of smectite diagenesis on sandstone cementation. *J. Sed. Pet.* **49**: 55-70.
- Brusewitz, A. M. 1986. Chemical and physical properties of Paleozoic potassium bentonites from Kinnekulle, Sweden. *Clays & Clay Miner.* **34**: 442-454.
- Chai, B. H. T. 1974. Mass transfer of calcite during hydrothermal recrystallization. In *Geochemical Transport and*

- Kinetics*. A. W. Hoffmann, B. J. Giletti, H. S. Yoder Jr., and R. A. Jund, eds. Washington: Carnegie Inst, 205–218.
- Christidis, G. 1992. Origin, physical and chemical properties, of the bentonite deposits from the Aegean Islands of Milos, Kimolos and Chios, Greece. Ph.D. thesis. Univ. Leicester, UK. 472 pp.
- Christidis, G., and A. C. Dunham. 1993. Compositional variations in smectites: Part I: Alteration of intermediate volcanic rocks. A case study from Milos Island, Greece. *Clay Miner.* **28**: 255–273.
- Christidis, G., and T. Marcopoulos. 1993. Kaolinite generating processes in the Milos bentonites and their influence on the physical properties of bentonites. *Bull. Geol. Soc. Greece* (in press).
- Christidis, G., P. W. Scott, and T. Marcopoulos. 1995. Origin of the bentonite deposits of Eastern Milos, Aegean, Greece: Geological, mineralogical and geochemical evidence. *Clays & Clay Miner.* **43**: 63–77.
- Eberl, D. D. 1978. The reaction of montmorillonite to mixed-layer clay: The effect of interlayer alkali and alkaline earth cations. *Geochim. Cosmochim. Acta.* **42**: 1–7.
- Eberl, D. D., G. Whitney, and H. Khoury. 1978. Hydrothermal reactivity of smectite. *Am. Miner.* **63**: 401–409.
- Eberl, D. D., and J. Srodon. 1988. Ostwald ripening and interparticle-diffraction effects for illite crystals. *Am. Miner.* **73**: 1335–1345.
- Eberl, D. D., J. Srodon, and H. R. Northrop. 1986. Potassium fixation in smectite by wetting and drying. In *Geochemical Processes at Mineral Surfaces*. J. A. Davis and K. F. Hayes, eds. Amer. Chem. Soc. Symp. Ser. **323**: 296–326.
- Eberl, D. D., J. Srodon, M. Kralik, B. E. Taylor, and Z. E. Peterman. 1990. Ostwald ripening of clays and metamorphic minerals. *Science* **248**: 474–477.
- Eberl, D. D., B. Velde, and T. McCormick. 1993. Synthesis of illite-smectite from smectite at earth surface temperatures and high pH. *Clay Miner.* **28**: 49–60.
- Fyticas, M. 1977. Geological and Geothermal and Study of Milos Island. Ph.D thesis. Univ. Thessaloniki, Greece, 228 pp. (in Greek).
- Fyticas, M., F. Innocenti, N. Kolios, P. Manetti, R. Mazzuoli, G. Poli, F. Rita, and L. Villari. 1986. Volcanology and petrology of volcanic products from the island of Milos and neighbouring islets. *J. Volcanol. Geotherm. Res.* **28**: 297–317.
- Glasmann, J. R., P. D. Lundegard, R. A. Clark, B. K. Penny, and I. D. Collins. 1989. Geochemical evidence for the history of diagenesis and fluid migration: Brent Sandstone, Heather Field, North Sea. *Clay Miner.* **24**: 255–284.
- Govindaraju, K. 1989. *Geostandards Newsletter* **13**: Spec. Issue, July 1989.
- Güven, N. 1974. Electron Optical investigations on montmorillonites-I. Cheto, Camp-Bertaux and Wyoming montmorillonites. *Clays & Clay Miner.* **22**: 155–165.
- Güven, N., and R. W. Pease. 1975. Electron Optical investigations on montmorillonites-II: Morphological variations in the intermediate members of the montmorillonite-beidellite series. *Clays & Clay Miner.* **23**: 187–191.
- Harvey, C. C., and P. R. L. Browne. 1991. Mixed-layer clay geothermometry in the Wairakei geothermal field, New Zealand. *Clays & Clay Miner.* **39**: 614–621.
- Howard, J. J., and D. M. Roy. 1985. Development of layer charge and kinetics of experimental smectite alteration. *Clays & Clay Miner.* **33**: 81–88.
- Hower, J., E. V. Eslinger, M. E. Hower, and E. A. Perry. 1976. Mechanism of burial metamorphism of argillaceous sediment: 1. Mineralogical and chemical evidence. *Bull. Geol. Soc. Am.* **87**: 725–737.
- Huang, W. L., J. M. Longo, and D. R. Pevear. 1993. An experimentally derived kinetic model for smectite-to-illite conversion and its use as a geothermometer. *Clays & Clay Miner.* **41**: 162–177.
- Huff, W. D., and A. G. Türkmenoglu. 1981. Chemical characteristics and origin of Ordovician K-bentonites along the Cincinnati Arch. *Clays & Clay Miner.* **29**: 113–123.
- Inoue, A., and M. Utada. 1983. Further investigations of a conversion series of diochahedral mica/smectites in the Shinzan hydrothermal alteration area, Northeast Japan. *Clays & Clay Miner.* **31**: 401–412.
- Inoue, A., N. Kohyama, R. Kitagawa, and T. Watanabe. 1987. Chemical and morphological evidence for the conversion of smectite to illite. *Clays & Clay Miner.* **35**: 111–120.
- Inoue, A., B. Velde, A. Meunier, and G. Touchard. 1988. Mechanism of illite formation during smectite-to-illite conversion in a hydrothermal system. *Am. Miner.* **73**: 1305–1334.
- Jagodzinski, H. 1949. Eindimensionale Fehlordnung in Kristallen und ihr Einfluss auf die Röntgeninterferenzen. I. Berechnung des Fehlorderungsgrades aus der Röntgenintensitäten. *Acta Crystallogr.* **2**: 201–207.
- Jahren, J. S. 1991. Evidence of Ostwald ripening related recrystallization of diagenetic chlorites from reservoir rocks offshore Norway. *Clay Miner.* **26**: 169–178.
- Kalogeropoulos, S. I. and P. Mitropoulos. 1983. Geochemistry of barites from Milos island (Aegean Sea), Greece. *N. Jb. Miner. Mh.* 13–21.
- Keller, W. D., R. C. Reynolds, and Inoue, A. 1986. Morphology of clay minerals in the smectite-to-illite conversion series by scanning electron microscopy. *Clays & Clay Miner.* **34**: 187–197.
- Lanson, B., and D. Champion. 1991. The I/S to illite reaction in the late stage diagenesis. *Am. J. Sci.* **291**: 473–506.
- Liakopoulos, A. 1987. Hydrothermalisme et mineralizations metalliferes de l' ile de Milos (Cyclades, Grece). Ph.D thesis. Univ. Pierre and Marie Curie, Paris, 276 pp.
- Lifshitz, I. M., and V. V. Slyozov. 1961. The kinetics of precipitation from supersaturated solid solutions. *J. Phys. Chem. Solids.* **19**: 35–50.
- Lindgreen, H., and P. L. Hansen. 1991. Ordering of illite-smectite in Upper Jurassic claystones from the North Sea. *Clay Miner.* **26**: 105–125.
- Mering, J., and A. Oberlin. 1971. The smectites. In *The Electron Optical Investigation of Clays*. J. A. Gard, ed. Mineralogical Society: London, 193–229.
- Muffler, P. L. J., and D. E. White. 1969. Active metamorphism of Upper Cenozoic sediments in the Salton Sea Geothermal Field and the Salton Trough, southeastern California. *Bull. Geol. Soc. Am.* **80**: 157–182.
- Nadeau, P. H., and R. C. Reynolds. 1981. Burial and contact metamorphism in the Mancos Shale. *Clays & Clay Miner.* **29**: 249–259.
- Nadeau, P. H., J. M. Tait, W. J. McHardy, and M. J. Wilson. 1984a. Interstratified XRD characteristics of physical mixtures of elementary clay particles. *Clay Miner.* **19**: 67–76.
- Nadeau, P. H., M. J. Wilson, W. J. McHardy, and J. M. Tait. 1984b. Interstratified clays as fundamental particles. *Science* **225**: 923–925.
- Nadeau, P. H., M. J. Wilson, W. J. McHardy, and J. M. Tait. 1984c. Interparticle diffraction: A new concept for interstratified clays. *Clay Miner.* **19**: 757–769.
- Newman, A. C. D., and G. Brown. 1987. The chemical constitution of clays. In *Chemistry of Clays and Clay Minerals*. A. C. D. Newman, ed. London: Mineralogical Society, 1–128.
- Ramseyer, K., and J. R. Boles. 1986. Mixed-layer illite/

- smectite minerals in tertiary sandstones and shales, San Joaquin Basin, California. *Clays & Clay Miner.* **34**: 115–124.
- Reynolds, R. C. 1989. Principles and techniques of quantitative analysis of clay minerals by X-ray powder diffraction. In *Quantitative Mineral Analysis of Clays*. D. R. Pevear and F. A. Mumpton, eds. CMS workshop lectures. **1**: 4–36.
- Robertson, H. E., and R. W. Lahann. 1981. Smectite to illite conversion rates: effects of solution chemistry. *Clays & Clay Miner.* **29**: 129–135.
- Rosenberg, P. E., J. A. Kittrick, and S. U. Aja. 1990. Mixed layer illite/smectite: A multiphase model. *Am. Miner.* **75**: 1182–1185.
- Singer, A., and P. Stoffers. 1980. Clay mineral diagenesis in two African lake sediments. *Clay Miner.* **15**: 291–307.
- Srodon, J. 1980. Precise identification of illite/smectite interstratifications by X-ray diffraction. *Clays & Clay Miner.* **28**: 401–411.
- Srodon, J., and D. D. Eberl. 1984. Illite. In *Micas*. S. W. Bailey ed. Washington D.C.: Mineralogical Society of America, **13**: 495–538.
- Srodon, J., D. J. Morgan, E. V. Eslinger, D. D. Eberl, and M. R. Karlinger. 1986. Chemistry of illite/smectite and end-member illite. *Clays & Clay Miner.* **34**: 368–378.
- Srodon, J., F. Elsass, W. J. McHardy, and D. J. Morgan. 1992. Chemistry of illite-smectite inferred from TEM measurements of fundamental particles. *Clay Miner.* **27**: 137–158.
- Steeffel, C. I., and P. van Cappellen. 1990. A new kinetic approach to modeling water-rock interaction: The role of nucleation, precursors and Ostwald ripening. *Geochim. Cosmochim. Acta* **54**: 2657–2677.
- Sucha, V., I. Kraus, H. Gerthofferova, J. Petes, and M. Serckova. 1993. Smectite to illite conversion in bentonites and shales of the East Slovak Basin. *Clay Miner.* **28**: 243–253.
- Veblen, D. R., G. D. Guthrie Jr., K. J. T. Livi, and R. C. Reynolds. 1990. High-resolution transmission electron microscopy and electron diffraction of mixed-layer illite smectite: Experimental results. *Clays & Clay Miner.* **38**: 1–13.
- Velde, B., and E. Nicot. 1986. Diagenetic clay mineral composition as a function of pressure, temperature and chemical activity. *J. Sed. Pet.* **55**: 541–547.
- Whitney, G. 1990. Role of water in the smectite-to-illite reaction. *Clays & Clay Miner.* **38**: 343–350.
- Whitney, G., and R. Northrop. 1988. Experimental investigation of the smectite to illite reaction: Dual reaction mechanisms and oxygen-isotope systematics. *Am. Miner.* **73**: 77–90.

(Received 27 June 1994; accepted 8 February 1995; MS 2528)